*Supplementary Materials*

# Novel Zr-rich alloys of ternary Ti-Zr-Nb system with large superelastic recovery strain

**Danil Barilyuk, Andrey Bazlov, Natalia Arkharova, Tatyana Teplyakova, Anton Konopatsky and Sergey Prokoshkin**

For the EDS analysis, three samples were prepared from each ingot (from the lower, middle and upper parts). To study the chemical composition, integral and pinpoint analysis was carried out over the selected area of the sample surface. Figure S1 collects the representative results of EDS studies: an electron image, the corresponding EDS profile, and elemental maps of the investigated alloy.

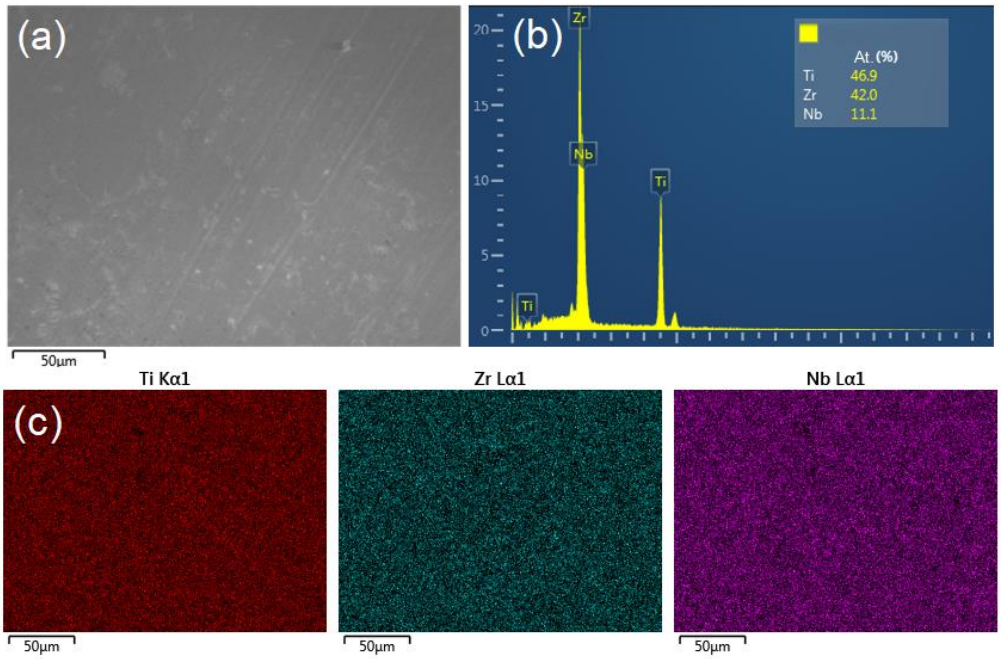


**Figure S1.** Chemical composition of theTi-42Zr-11Nb alloy; (**a**) electron image, (**b**) EDS spectra, (**c**) elemental maps.

It can be seen from the presented integral spectra that the obtained chemical composition of the bottom of the Ti-42Zr-11Nb alloy ingot is in good agreement with the nominal one. The obtained maps of the elements distribution demonstrate that the main components of the alloy are distributed evenly throughout the ingot. Similar results were obtained for all investigated alloys.

Table S1 shows a comparison of the nominal chemical composition of the alloys with the obtained one. "Point" means a small area of about 5 μm².

**Table S1.** Comparison of nominal and actual chemical compositions.

| **Nominal, %** | | | **Integral, %** | | | **At point, %** | | |
|---|---|---|---|---|---|---|---|---|
| Ti | Zr | Nb | Ti | Zr | Nb | Ti | Zr | Nb |
| 47 | 41 | 12 | 46,2 ± 0,6 | 41,4 ± 0,5 | 12,3 ± 0,2 | 46,8 ± 1,0 | 40,9 ± 0,7 | 12,2 ± 0,5 |
| 47 | 42 | 11 | 46,9 ± 0,6 | 42,0 ± 0,3 | 10,8 ± 0,2 | 47,6 ± 0,9 | 41,6 ± 0,9 | 10,8 ± 0,6 |
| 47 | 43 | 10 | 47,4 ± 0,7 | 42,7 ± 0,5 | 9,9 ± 0,3 | 46,7 ± 0,9 | 43,5 ± 0,8 | 9,8 ± 0,6 |
| 46 | 44 | 10 | 45,3 ± 0,6 | 44,3 ± 0,4 | 10,4 ± 0,3 | 46,2 ± 1,0 | 43,6 ± 0,7 | 10,2 ± 0,5 |

Table S1 confirms that actual chemical composition of alloys is in good agreement with the nominal one.

Figure S2 shows XRD profile of 41-12 alloy after TMT and additional CR of 10%.

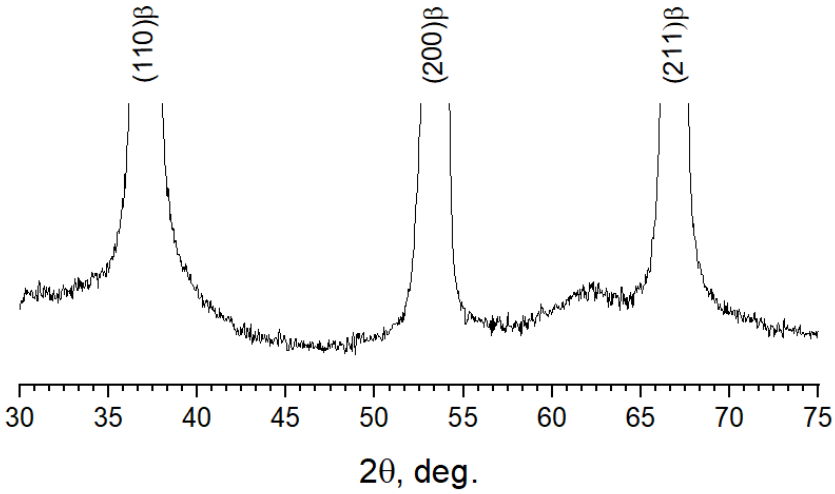


**Figure S2.** XRD profile of 41-12 alloy after TMT and additional CR of 10%.

There are no clearly distinguishable martensite peaks, which means that in case of 41-12 alloy, additional 10% of plastic deformation is not enough to induce martensitic transformation.

Figure S3 depicts DSC curves for all obtained materials subjected to TMT.

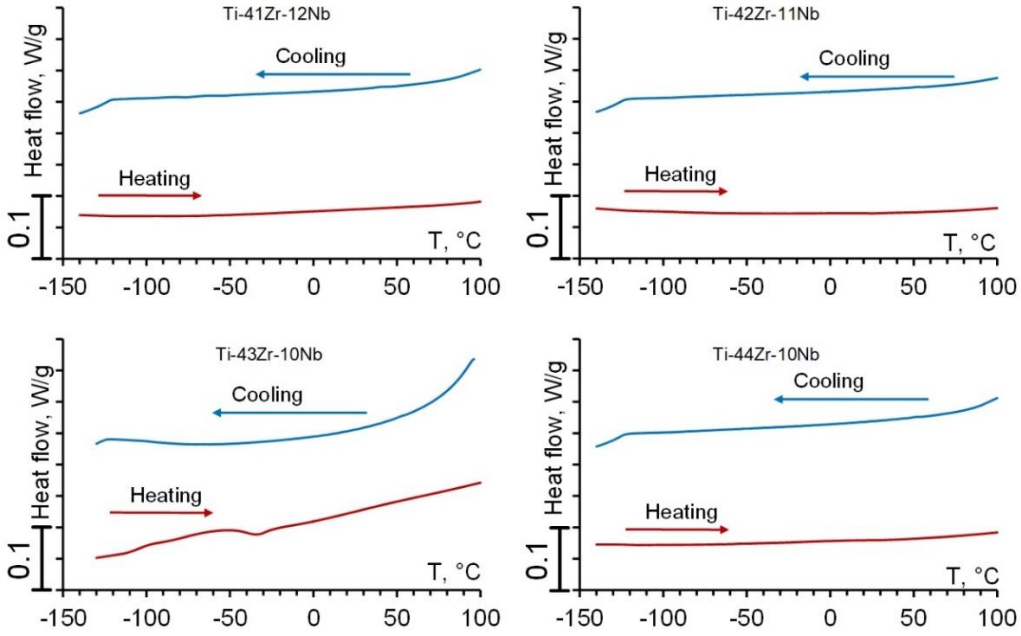


**Figure S3.** DSC curves for the studied alloys after TMT.

According to the heat flow curve neither an exothermic maximum nor an endothermic minimum was observed. The absence of the vivid heat effect of martensitic transformation in some Ti-Zr-Nb alloys was also observed in [1]. Such phenomenon can be sue to a small enthalpy of martensitic transformation and concurrent $\omega$-phase formation.

Additional mechanical testing scheme was used in order to assess superelastic recovery strain of the obtained materials. For that each sample was loaded up to 6% of tensile deformation then unloaded down to zero stress. Obtained stress-strain curves are given in Figure S4.

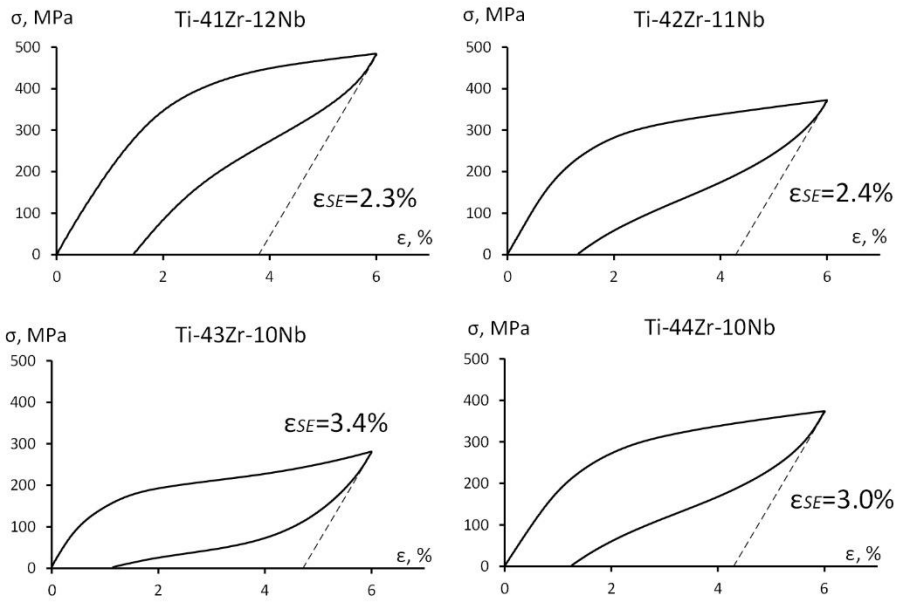


**Figure S4.** Stress-strain curves of the obtained alloys loaded up to 6% of tensile deformation.

It this case alloys with higher Zr and lower Nb content demonstrate considerably higher superelastic recovery strain. These results can be associated with the fact that alloys with higher Nb concentration require some mechanical training for demonstration of more pronounced superelasticity due to more stable parent phase.

## References

[1] Q. Liang, D. Wang, Y.. Zheng, S. Zhao, Y. Gao, Y. Hao, R. Yang, D. Banerjee, H. L. Fraser, Y. Wang Shuffle-nanodomain regulated strain glass transition in Ti-24Nb-4Zr-8Sn alloy, Acta Materialia 186 (2020) doi.org/10.1016/j.actamat.2019.12.056